Synthesis and characterization of cellulose hydrogel/graphene oxide/polyaniline composite for high-performing supercapacitors

Marwa Ben Hadj Said, Khaled Charradi, Zakarya Ahmed, Hubert Cachet, Catherine Debiemme-Chouvy, Qana Alsulami, Sami Boufi, Sherif Keshk, Radhouane Chtourou

Synthesis and characterization of cellulose hydrogel/graphene oxide/ polyaniline composite for supercapacitors

Marwa Ben Hadj Said[ab], Khaled Charradi*[b], Zakarya Ahmed[b], Hubert Cachet[c], Catherine Debiemme-Chouvy[c], Qana A. Alsulam[d], Sami Boufi[e], Sherif M.A.S. Keshk[b], Radhouane Chtourou[b]

[a] Nanomaterials and Systems for Renewable Energy Laboratory, Research and Technology Center of Energy, Technopark Borj Cedria, BP 095 Hammam Lif, Tunisia.

[b] University of Sousse, High School of Sciences and Technology of Hammam, Sousse, Tunisia

[c] Laboratoire Interfaces et Systèmes Electrochimiques, UMR 8235, CNRS, Sorbonne Université, 4 place Jussieu, 75005 Paris, France

[d] Chemistry Department, Faculty of Science, King Abdulaziz University, 21589, Jeddah, Saudi Arabia

[e] University of Sfax- LMSE-Faculty of Science-BP 802-3018, Sfax, Tunisia

***Corresponding author:** Khaled Charradi, charradikaled2010@gmail.com

Abstract

We have synthesized a ternary composite electrode comprising graphene oxide (GO), cellulose hydrogel and polyaniline (PANi). The composite deposited on a platinum electrode was electrochemically characterized. It was investigated using cyclic voltammetry (CV), galvanostatic charge-discharge (GCD) and electrochemical impedance spectroscopy (EIS). The ternary composite electrode showed significantly enhanced cycling stability and improved areal capacitance of 500-600 $F \cdot g^{-1}$ indicating a synergistic effect of cellulose hydrogel on PANi-GO. We believe the results of this study provide a strong experimental basis for the functioning of supercapacitors.

Highlights

- A cellulose hydrogel/GO/PANi composite was synthesized using the polymerization method.
- Cellulose hydrogel is crucial for the functioning of the composite.
- Cellulose hydrogel composite exhibits superior performances.

Keywords: Polyaniline, graphene oxide, cellulose hydrogel, supercapacitor

1. Introduction

Supercapacitors (SCs) are storage devices that store electrochemical energy. The stored energy is used via reversible adsorption and desorption of particles at the connection points between electrode materials and electrolytes.[1-3] The functioning of SCs completely depends on the type of electrode materials rather than electrolytes. Presently, two kinds of electrode materials are used in SCs, namely carbon-based materials with an electric twofold layer feature and materials with a pseudocapacitive component that executes electron movement and charge storage via redox reactions.[4] Polyaniline (PANi), a type of superior pseudo capacitance resource, is used with advantages of cost-effectiveness, facile synthesis, and high conductivity.[5] PANi endures high specifc capacitance, high specifc controlled by the doping stages.[6-9] Though, the structures and properties of PANi have to deal with the synthesis conditions because of the complexities in molecular structure. Additionally, features including its humidity, temperature, pH, electrochemical redox state, and the sort of anions in the solution infuence its conductivity.[10-14] However, one of the major disadvantages associated with the use of PANi is poor cycling performance. Thus, to enhance the efficiency of SCs, carbon-based materials with PANi composites are now being used. Synergistic and complementary properties of the composites based on PANi and graphene oxide (GO) with concern to their potential applications in sensors,[15-19] supercapacitors,[7,19,20] alcohol dehydration [21-22] and adsorbents,[23–30] have attracted considerable attention.

Recently, an increasing number of studies have been conducted for the controlled synthesis of graphene/PANi composites.[31] The graphene/PANi composite can overcome the poor cycling performance of PANi; in addition, it provides a synergistic electric effect of a twofold layer and pseudocapacitance.[32] PANi-coated graphene fibers exhibit the highest specific capacitance (480 $F \cdot g^{-1}$ at 0.1 $A \cdot g^{-1}$), whereas the reduced graphene oxide rGO-PANi electrode displays a capacitance of only 286 $F \cdot g^{-1}$ after 2000 cycles.[33] The need of low costand biodegradable materials in hardware has been fundamentally expanded with the increase in warming and energy emergency. Currently, studies are being conducted to develop highly flexible, free-standing, and binder-free electrodes using cost-effective and renewable polymeric materials.[34] A cellulose biopolymer with its remarkable supramolecular structure and fabric properties can be used for conducting polymers. PANi was synthesized via a polymerization reaction using dispersed cellulose to form the PANi–cellulose composite that was applied as a conducting paper sheet.[35,36] The scope for further derivatization, rigid oriented molecular structure, inherent strength, stability, and film-forming properties provide a complementary characteristic to cellulose in the conductive polymers as PANi.[37] Native cellulose has a high resistivity and can provide superior energy and mechanical homogenization of raw materials.[38] This procedure modifies the surface presentation such that fibrils are enclosed in the matrix, resulting in a large contact area among the microfibrils, thus increasing the resistance. Cellulose hydrogel has been increasingly used to fabricate smart devices because of their overall biocompatibility, high storage capacity for cells and small molecules, and low interfacial tension at the gel–aqueous solution interface.[39] The properties of cellulose hydrogels need to be adjusted to synthesize flexible, elite execution practical materials.[40] Unfortunately, films synthesized from PANi and microcrystalline cellulose are dissolvable in N,N-dimethylacetamide (DMAc)/lithium chloride (LiCl) (9%) solutions; these display no conductive behavior after cellulose regeneration and drying.[41] In contrast, a ternary composite electrode consisting of microcrystalline cellulose

treated with 9 to 15% carboxymethyl cellulose and PANi exhibited high conductivity when the percentage of PANi in the binary composite was reduced from 50 to 33%.[42] However, films with 17 and 9% PANi showed no conductance. As a framework of modified electrodes, the cellulose/graphene oxide (GO) composite is incorporated into PANi nanoclusters via the polymerization. The ratio of GO and PANi is adjusted so that the ternary cellulose/GO/PANi membrane displays specified three-dimensional porous structures and high conductivity (1.15 S/cm) because of its good specific capacitance of 1218 mF/cm^2.[43] In the present study, we studied the effect of incorporating cellulose hydrogel into the GO/PANi matrix to achieve a more prominent conductive composite with a high explicit surface. The novelty of the current research is the facile method used to add GO and cellulose hydrogel during the synthesis of PANi to enhance its conductivity for high-performing SCs. The findings of the study obtained for the tertiary composite are interessant for the functioning of SCs. In addition, the charge–discharge obtained from the prepared composite is considered a component of the SC framework.

2 EXPERIMENTS

2.1 Materials

All chemicals used were of analytical grade. Aniline (99.9%, monomer), ammonium persulfate ($[NH_4]_2S_2O_8$, 98%), graphite powder, microcrystalline cellulose, $KMnO_4$, ethanol, deionized water, $NaNO_3$, H_2O_2, $(NH_4)_2S_2O_8$, potassium permanganate (99%, RFCL), H_2O_2 (40% wt., EMPLURA), H_2SO_4, (98%, ACS), HCl (35%, RANKEM).

2.2 Synthesis of graphene oxide

Graphene oxide (GO) was synthesized from graphite powder using Hummer's method after modification.[1] Briefly, graphite powder (2 g) and $NaNO_3$ (2 g) were added to H_2SO_4 (90 mL) in an ice bath. Next, $KMnO_4$ (12 g) was gradually added with stirring at 40 °C for 30 min. Deionized water (90 mL) was subsequently added slowly to the mixture, followed by the

addition of 30% H_2O_2 (10 mL). The product was extracted by centrifugation and washed repeatedly with 5% HCl solution until the pH became neutral.

2.3 Synthesis of graphene oxide/cellulose hydrogel

First, a solvent exchange activation pretreatment was performed to diminish the hydrogen bonds among the cellulose chains to achieve a relaxed conformation. The pretreatment was performed as follows: cellulose was suspended in water for 1 h; the water was removed and replaced by methanol, and then by dimethylacetamide (DMAc), with a change of each solvent after 1 h. Finally, the cellulose was filtered and dried at 70 °C. A typical preparation procedure for 1 wt. % cellulose solution was as follows: activated cellulose (1 g) was added to the LiCl/DMAc solvent and stirred to form a uniform suspension GO/cellulose (1/10, unless otherwise stated) by ultrasonication for 1 h.[44]

2.4 Synthesis of cellulose hydrogel/GO/PANi composite by polymerisation

The cellulose hydrogel/GO/PANi composite was prepared via *in situ* chemical polymerization of aniline (ANi) on the cellulose/GO sheet, in which, 100 mL of ANi (4.16 mM) and HCl (1.0 M) were continuously stirred in an ice bath for 4 h. Afterward, $[NH_4]_2S_2O_8$ was added. The obtained composite was washed with ethanol and deionized water.

2.5 Electrochemical characterizationsof the composite

The composites were electrochemically studied using a three-electrode setup. The composite coated platinum, a Pt grid (S = 2 cm^2) and an Ag/AgCl electrode were used as the working, counter, and reference electrodes, respectively. The three electrodes immersed in H_2SO_4 (1 M) were studied using cyclic voltammetry (CV), galvanostatic charge/discharge curves (GCDs), and electrochemical impedance spectroscopy (EIS) (Solartron Analytical).

2.6. Characterization

Reference PANi, PANi/GO and composite electrodes were investigated using several techniques. The FTIR spectra were measured using Bruker Optics (FT-IR IFS 66S Vacuum, Germany) spectrophotometer (500–4000 cm^{-1}) by diluting the filler powder (1 wt.%) in potassium bromide (KBr) pellet. The X-ray diffractograms were recorded using the automated Bruker D8 advance X-ray diffractometer with CuKα radiations (40 kV and 30 mA) at 2θ values over 5 to 50°. Samples were used in the form of compressed tablets. The scanning electron microscopy (SEM) micrographs were obtained from a field emission gun scanning electron microscope (FEG-SEM), Ultra55 Zeiss, operating at 5 kV.

RESULTS AND DISCUSSION

3.1 FTIR

Figure 1 shows the FTIR spectra of PANi, GO/PANi, and cellulose hydrogel/GO/PANi. The principal characteristic band locations of PANi and their composites were almost same, with a single broad weak band at 3200 cm^{-1} that corresponded to the N–H stretching vibration, whereas the stretching vibration of the aromatic C-H bond corresponded to 2995 cm^{-1} (Fig. 1).[45]

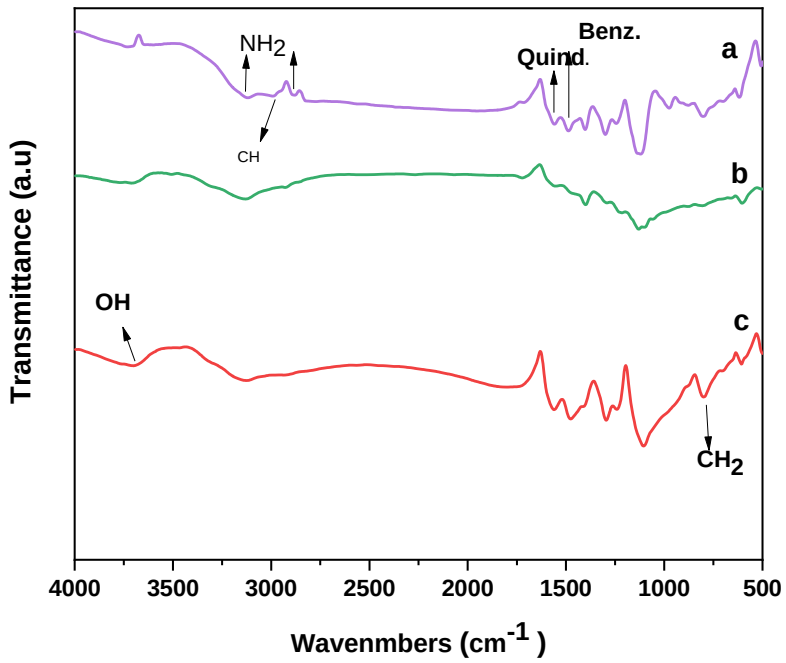

FIGURE 1 FTIR spectra of (a) PANi, (b) GO/PANi, and (c) cellulose hydrogel/GO/PANi.

The two bands at 1558 cm^{-1} and 1488 cm^{-1} corresponded to the stretching vibrations of the quinoid and benzenoid rings, respectively. The peak at 1400 cm^{-1} was attributed to the C–N stretching vibration between benzenoid and quinoid units.[46] The band at 1299 cm^{-1} corresponded to the π-electron delocalization through the C-N-C stretching vibration, whereas the characteristic band of C-N^+ stretching vibration in the polaron structure was present at 1242 cm^{-1}.[47] The broad band at 1124 cm^{-1} was assigned to the aromatic C-H bending in the plane for the 1,4-disubstituted aromatic ring.[1] In the FTIR of GO/PANi, the prominent bands observed in pristine PANi were retained in the composite with weak intensity, whereas the characteristic bands of GO disappeared owing to the chemical interaction between graphene and the carboxyl group and the nitrogen of the polyaniline backbone.[48]The interaction of graphene with imine groups (C=N) in the quinonoid ring of polyaniline was confirmed by the broadness and shifting of the initial position of the band from 1558 to 1567 cm^{-1}. In the FTIR of the ternary composite, the major bands observed in pristine PANi appeared with characteristic bands of cellulose

hydrogel at 3600 cm^{-1} corresponding to the hydroxyl group stretching vibration. It could be attributed to the graft crosslinking reaction of graphene, polyaniline, and cellulose hydrogel via hydrogen bonding.[48]

3.1. X-Ray diffraction

Along with FTIR spectroscopy, X-ray diffraction was used to provide a detailed understanding of the ordered structures of the GO/PANi and cellulose hydrogel/GO/PANi. The XRD patterns of GO, cellulose hydrogel, and the ternary composite are illustrated in Fig. 2. In the absence or weak interaction between PANi and GO or cellulose hydrogel in the composite, each component showed its crystallinity peaks in the composite. No diffraction peak of GO was observed in GO/PANi and cellulose hydrogel/GO/PANi composites, suggesting that GO was dispersed and absorbed well in the PANi structure.

However, the principal peak of GO/PANi at $2\theta = 25.36°$ was slightly sharper than that of PANi, which was attributed to the reconstruction of the PANi sheet, owing to the regular stacking of GO (Fig. 2).

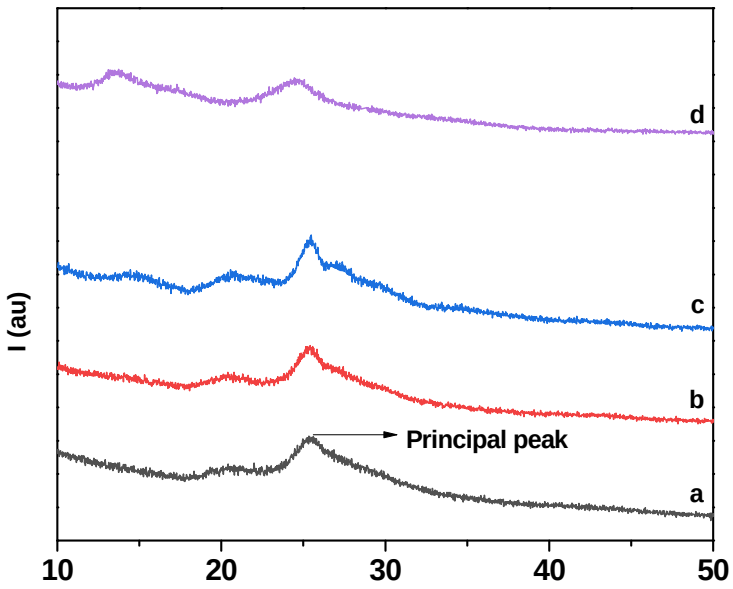

FIGURE 2 XRD of **a.** PANi, **b.** GO/PANi, **c.** cellulose hydrogel/GO/PANi, and **d.** cellulose hydrogel.

The XRD pattern of cellulose hydrogel presented two broad peaks at 2θ = 13.6° and 24.7° reveals the formation of cellulose I in the cellulose hydrogel.[48] In addition, the broadness demonstrates the destruction of the cellulose crystalline structure by forming cellulose hydrogel, implying the breaking of hydrogen bonds during the dissolution process and regeneration of cellulose structure after the removal of the solvent. The incorporation of PANi into the cellulose hydrogel/GO/PANi composite was confirmed by a slight sharp in the principal peak with a minor shift in the peak to the lowest angles, indicating an increase in the crystallinity in the ternary composite (Fig. 2).

The cellulose peaks were less visible in the composite, which was presumably attributed to the low content of cellulose in the film and the crystallite size of regenerated cellulose, thereby broadening the diffraction peak.

3.3 Scanning electron microscopy

The SEM micrographs of GO/PANi exhibits the formation of a spongy irregular agglomerated structure (Fig. 3a).[49] The SEM study of the cellulose hydrogel/GO/PANi showed the presence of cellulose hydrogel particles enclosed by GO/PANi chain agglomerates (Fig. 3b). The microstructure of the ternary composite displays the existence of modified aggregate porous regions that may facilitate an electrical sensing response.

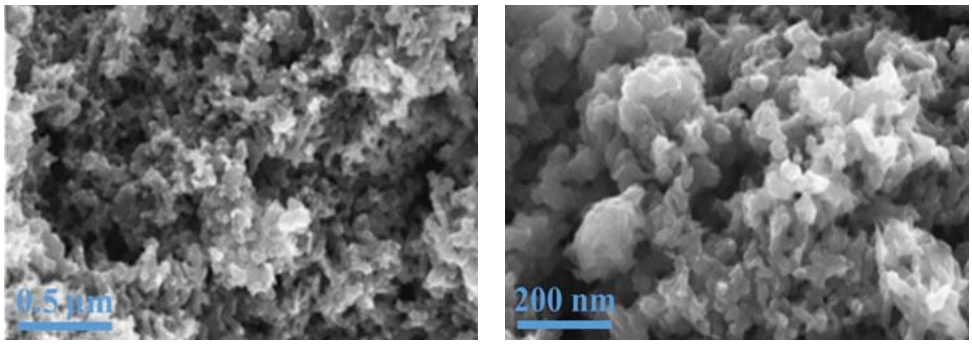

a

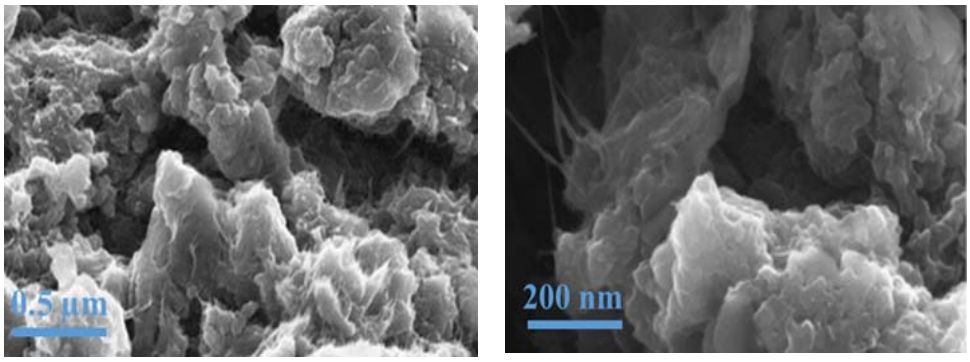

b

FIGURE 3 SEM micrographs of **a**. GO/PANi and **b**. cellulose hydrogel/GO//PANi.

3.4 Electrochemical characterization

3.4.1. Cyclic voltammetry

Cyclic voltammetry was performed using a three-electrode cell (Ag/AgCl reference electrode, a platinum auxiliary electrode, and a coated platinum electrode). The CV curves were obtained using 1M H_2SO_4 as electrolyte, which was used for measuring the gravimetric and real capacitance of the electrodes. The comparison of the voltammograms of GO/PANi and cellulose hydrogel/GO/PANi shows clearly that the presence of cellulose hydrogel in the composite allows to obtain higher current intensity (Fig. 4 curves b and c).

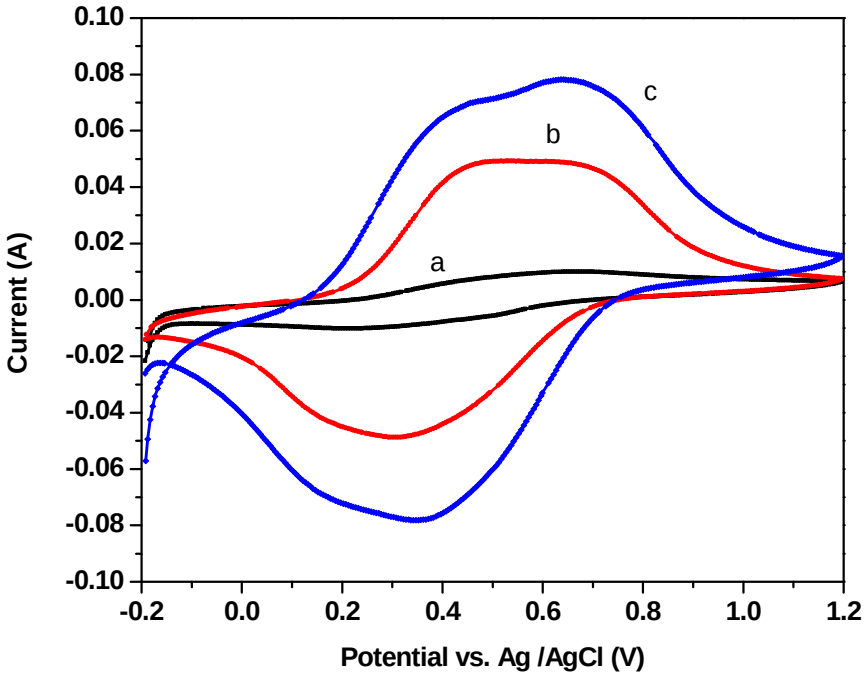

FIGURE 4 Cyclic voltammograms of a. PANi , b. PANi-GO, c. cellulose hydrogel/GO/PANi in 1 M H_2SO_4, at 50 mV/s.

These results confirmed the importance of cellulose hydrogel. It favors water absorption and water retention because of its porous structure; in addition, it behaves as an electrolyte reservoir [50] that allows fast proton movement for cellulose hydrogel/GO/PANi at the current intensity and surface air in voltammograms, confirming good rate capability of the ternary composite electrode and revealing their typical capacitive behaviors.[50,51] The comparative evaluation of different cellulose hydrogel ratios present in the composite is shown in Fig. 5.

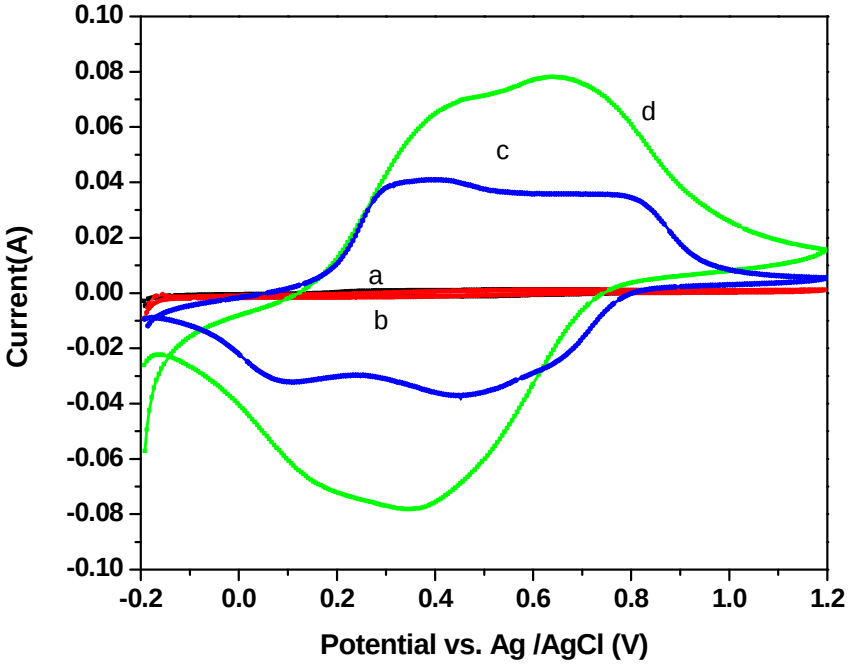

FIGURE 5 Cyclic voltammograms at 50 mV/s of cellulose hydrogel/GO/PANi for different percentages of cellulose hydrogel. a. 1/10, b. 1/5, c. 1/1, d. 1/2, in 1 M H_2SO_4.

The best ratios that provided a high intensity were 1/1 and 1/2 ratios. The fine electrochemical performance of the cellulose hydrogel could be ascribed to its interfacial property and electrolyte diffusion rate. The difference in the anode and cathodic strengths in terms of scanning speed confirmed the electrolyte diffusion of cellulose hydrogel (Fig. 6).

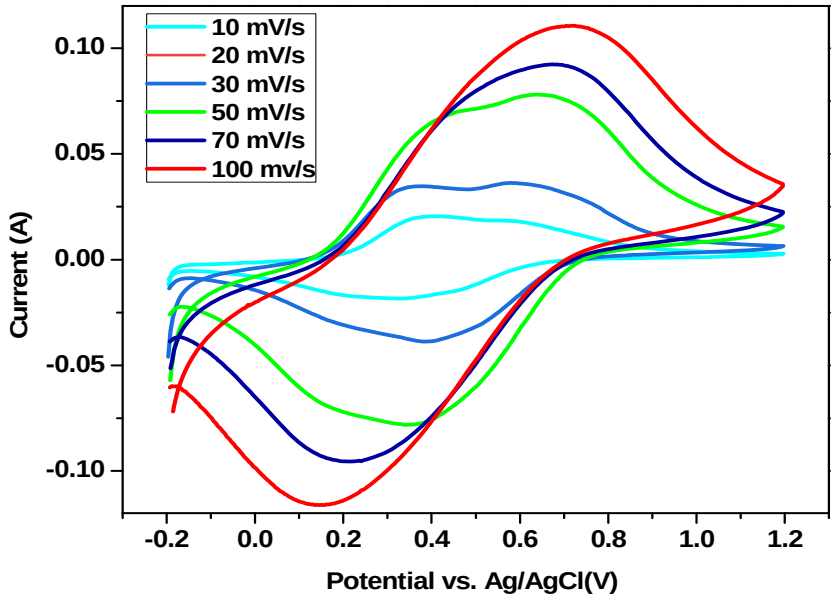

FIGURE 6 Cyclic voltammetry responses at different scan rates, in 1 M H_2SO_4 solution.

The cyclic curve of the ternary composite at various scan rates (ranging from 10 to 100 $mV \cdot s^{-1}$) enabled the movement of anodic peaks to higher potentials, and cathodic peaks move to lower potentials, owing to a slight increase in the resistance of the electrode at great sweep rates.[50] Figure 6 shows the cyclic curves of the composite at a scan rate varying from 10 to 100 $mV \cdot s^{-1}$. All cyclic curves describe a non perfect rectangular shape, indicating a diffusion limited reversible capacitive performance of the system. In addition, the shape of the cyclic curve was well maintained even at a higher scan rate of 100 $mV \cdot s^{-1}$ (Fig. 6), showing its good performance.[50] At 100 $mV \cdot s^{-1}$ the cathodic peak current is about 120 mA. This allows us to estimated a specific capacitance of 600 $F \cdot g^{-1}$.

3.4.2. Galvanostatic charge–discharge

Charge–discharge is one of the essential techniques to determine the performance of an SC. The GCD plots of cellulose hydrogel/GO/PANi at several constant load currents in the potential ranged from 0.0 to 0.8 V and are shown in Fig. 7.

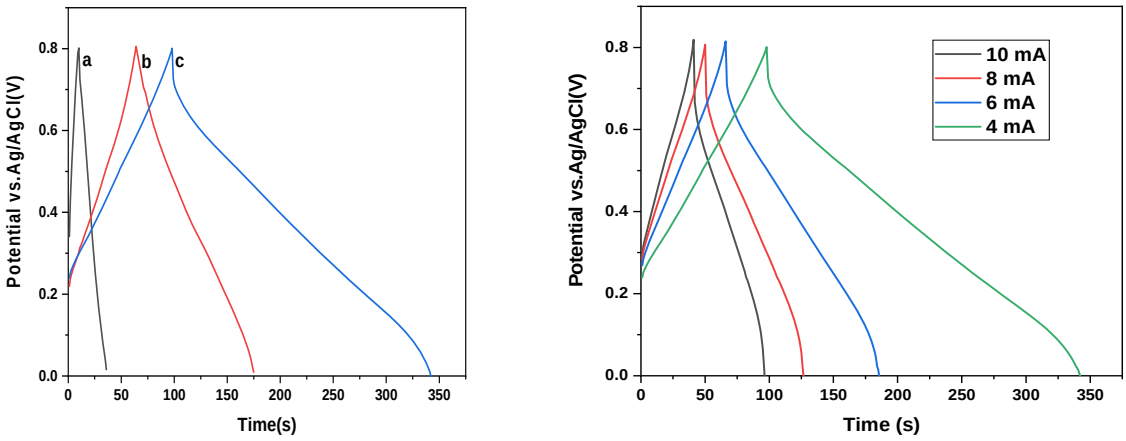

FIGURE 7 **(A)** GCD of PANi (**a**), GO/PANi (**b**), and cellulose hydrogel/GO/PANi (**c**) at 4 mA. (**B**) GCD of cellulose hydrogel/GO/PANi at different currents.

The curve charge reflects the pseudocapacitive quality of the modified electrode and significant performance. Symmetrical GCD curves confirmed the excellent supercapacitor material at low voltage owing to the high coulomb efficiency. As shown in Fig. 7, the GCD of the ternary composite decreased with the increase in the charge–discharge current density. The discharge capacitance of the ternary composite took more time than PANi or GO/PANi, suggesting that the ternary composite had good rate capability, owing to the presence of cellulose hydrogel, the mass of the active material was about 2 mg that was significant for the electrode material of an SC to deliver a high power density.

In contrast, the specific capacitance (C) of the ternary composite was calculated from GCD curves using equation (1):

$$C = \frac{I\,\Delta t}{m\,\Delta v} \qquad (1)$$

where I is the discharge current, Δt is the discharge time, m is the mass of active material, and Δv is the potential difference for discharging. The specific capacitance of the cellulose

hydrogel/GO/PANi composite was around 620 $F \cdot g^{-1}$ at a current density of 2 $mA \cdot cm^{-2}$. The current density increases as the specific capacitance decreases due to the diminished mobility of protons compared to that of electrons. A study of the stability of the electrode showed that the capacitance maintained the performance of up to 85% after 700 charge/discharge cycles (Fig. 8).

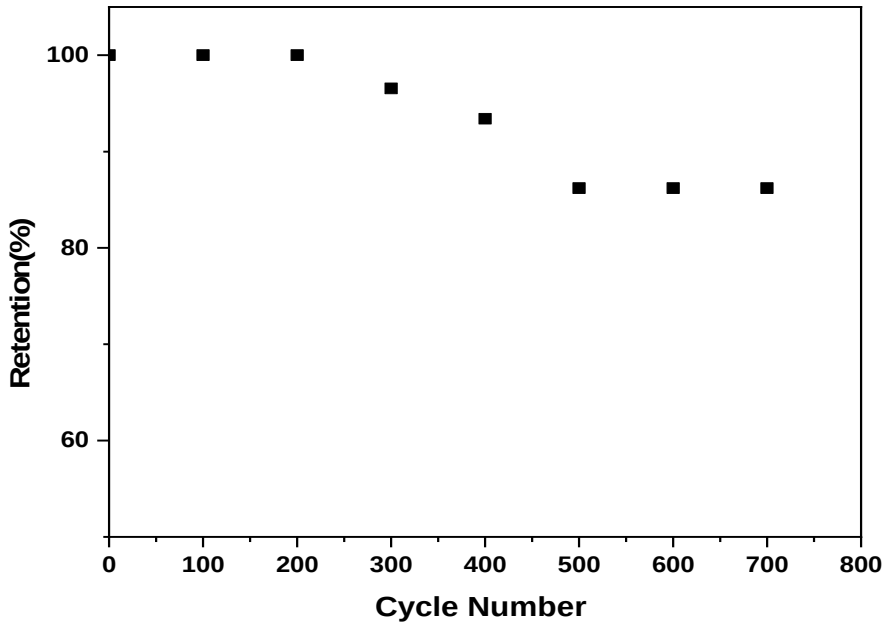

FIGURE 8 Variation of the capacitance of cellulose hydrogel/GO/PANi with the number of cycle.

It can be attributed to the incorporated cellulose hydrogel that hinders the reduction in the volume and extension of the PANi/GO matrix through the charge and discharge process.

The cellulose hydrogel/GO/PANi showed enhanced supercapacitor properties with the highest specific capacitance of 600 $F.g^{-1}$ at 4 mA and 85% capacity retention after 700 cycles in 1 M H_2SO_4 aqueous electrolyte. Our electrochemical results are in a good position compared with previous studies reported recently (Table 1). In different studies hydrogels of cellulose or

bacterial cellulose with capacities about 1035 and 4160 mF/cm², the capacitance is very low compared to our work. In another work authors used aerogel polyaniline and cellulose hydrogels[43] to have more capacitance and performance. *Other author used hydrogel polymer (polyvinyl alcohol)[53] or oxide [1, 52] were the capaciatnace is more than 700 F/g.*

Table 1 : Comparison of the electrochemical performance for Electrode based polyaniline

Electrode	Specific capacitance at current density or scan rate	References
Polyaniline@graphene@bacterial cellulose	4.16 $F.cm^{-2}$ at 1.0 mA/cm^2	50
polyaniline@cellulose hydrogels	1003.50 mF/cm^{-2} at 1.0 mA/cm^2	51
Polypyrrole@cellulose hydrogels	255 $F.g^{-1}$ at 0.25 $A.g^{-1}$	44
Polyaniline@GO@Hydrogel cellulose	600 $F.g^{-1}$at 2 mA/cm^2	This Work

3.4.3. Electrochemical impedance spectroscopy (EIS)

In order to get an estimate of the electrical capacitance of the PANi, PANi/GO and cellulose hydrogel/GO/PANi composite films, electrochemical impedance spectroscopy measurements were performed at room temperature, at the rest potential, in 1 M H_2SO_4 solution. The obtained impedance spectra are depicted in Fig.9A, as Nyquist plots in the (Z', Z") complex plane. They are characterized by a quasi semi-circular capacitive loop at frequencies above a few Hertz and a more or less linear vertical branch at lower frequencies. For every films, the capacitive loop can be attributed to the bulk dielectric and conductive properties of the polymeric matrix. This was represented by the parallel combination of a resistance and a constant phase element (CPE), $Q = Q_0(j\omega)^n$, accounting for a non ideal capacitance due to roughness or/and porosity effects, ω being the pulsation. The low frequency part of the three spectra is governed by the diffusion of charged species at the film/solution interface, but with a significant difference between them. For the PANi film, a 45° slope is evidenced, characteristic of a bulk, plane, infinite diffusion process, formally represented by a Warburg impedance W(ω) as $W = Z_0/(j\omega)^{0.5}$. For the two other films, the low frequency branch is much more vertical which suggests that diffusion

occurs in a limited space with the boundary condition of a blocking interface. Such a behavior is classically represented by a diffusion impedance T(ω) as $T = Z_0.\coth[B(j\omega)^{0.5}]/(j\omega)^{0.5}$. On the basis of the above considerations, the experimental EIS spectra were analyzed by means of electrical equivalent circuits given in Table 1, minimizing as possible the number of adjustable parameters. The fitting process was performed using the ZsimWin^{TM} software. The fitted parameters are reported in Table 1 and the fit quality is illustrated in Fig. 9B,C,D.

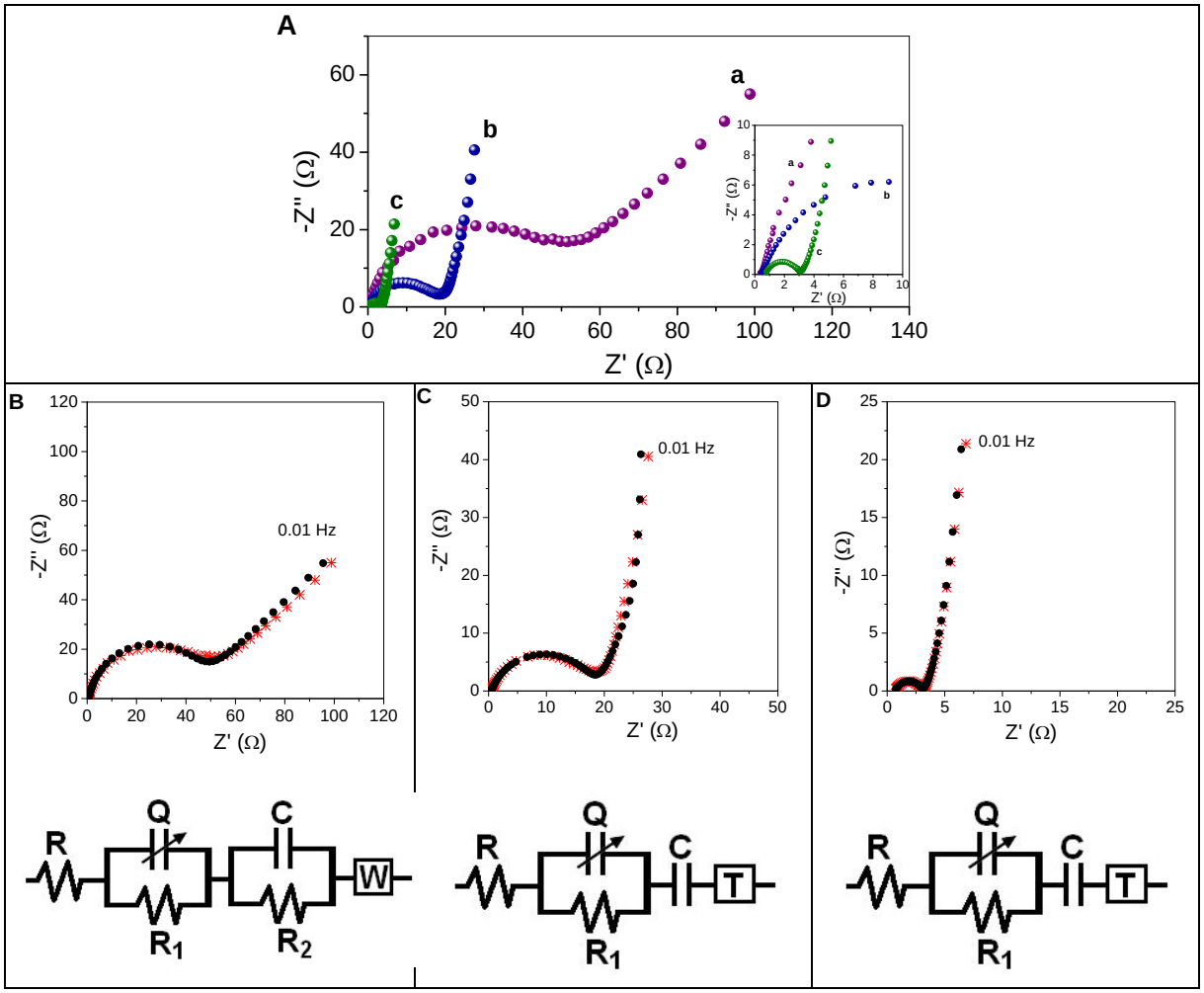

FIGURE 9 Nyquist plots of (**a, B**) PANi, (**b, C**) GO/PANi, (**c, D**) cellulose hydrogel/GO/PANi coated Pt electrodes in 1 M H_2SO_4. (A) experimental data. (B,C,D) experimental data (black circle) and fitted data (red cross). Equivalent circuits used to fit the experimental data.

TABLE 1 Equivalent circuits and fitted values for the different samples.

Sample	Equivalent circuit	R Ω	R_1 Ω	Q $\Omega^{-1}s^n$	n	R_2 Ω	C mF	Z_0 $\Omega\ s^{-0.5}$	B $S^{0.5}$
PANi	$R(R_1Q)(R_2C)W$	0.32	27	0.00443	0.945	14.7	**2.05**	19.2	-
PANi/GO	$R(R_1Q)CT$	0.44	17	0.00122	0.776	-	**548**	4.16	6.4
HC/GO/ PANi	$R(R_1Q)CT$	0.71	2.3	0.00067	0.78	-	**913**	1.19	13.9
			Bulk polymeric matrix			**Interface**		**Bulk diffusion**	

The dielectric properties of the polymeric matrix of composite PANi films are strongly affected with respect to the pristine PANi film. For both composite samples, the film resistance is decreased, reaching a factor of ten for the cellulose hydrogel/GO/PANi sample. The film capacitance, almost ideal for the pristine PANi, deviates notably from ideality for the composite PANi films, with a CPE exponent (n) of 0.78. As evidenced by the SEM micrographs, this behavior can be assigned to the strong porosity of the composite films. Another consequence of the increase in porosity is the decrease of the amplitude (Z_0) of the diffusion impedance, counterbalanced by a marked increase in the diffusion time (given by B^2) reaching about 40 s for PANi/GO and about 200 s for cellulose hydrogel/GO/PANi. The last but the most important parameter in view of the SC application is the interfacial capacitance C. For the pristine PANi film, C lies around 2 mF. It becomes 548 mF for PANi/GO and reaches 913 mF for cellulose hydrogel/GO/PANi leading to a specific capacitance around 500 $F \cdot g^{-1}$ in good agreement with the previous results. These results demonstrate the efficiency of the proposed strategy for obtaining very large capacitance values on the basis of a PANi film.

4 CONCLUSIONS

A cellulose hydrogel/GO/PANi composite was successfully synthesized for SCs and investigated. The composite was produced using a facile method by adding GO and PANi to

increase the conductivity and enhance the specific surface area of the prepared composite for the application of SCs. The presence of cellulose hydrogel improved the performance of SC, specific capacitance, and capacitance retention after 700 cycles.

REFERENCES

1. Kathalingam A, Ramesh S, Yadav HM, Choi J-H, Kim HS, Kim H-S. Nanosheet-like $ZnCo_2O_4$@ nitrogen doped graphene oxide/polyaniline composite for supercapacitor application: effect of polyaniline incorporation. *J Alloys Compd*. 2020; **830**:154734.
2. Xihong Lu,Minghao Yu, Gongming Wang, Yexiang Tong, Yat L. Flexible solid-state supercapacitors: design, fabrication and applications. Energy Environ Sci.2014; **7:** 2160-2181.
3. Yaseen M, Khattak MAK, Humayun M, Usman M, Shah SS, Bibi S, Hasnain BSU, Ahmad SM, Khan A, Shah N, Tahir AA, Ullah H. A Review of Supercapacitors: Materials Design, Modification, and Applications. *Energies*. 2021; **14:**7779.
4. Hong X, Fu J, Liu Y, Li S, Wang X, Dong W, Yang S. Recent Progress on Graphene/Polyaniline Composites for High-performance Supercapacitors. *Materials*. 2019; **12**:1451.
5. Kathalingam A, Ramesh S, Sivasamy A, Kim H S, Kim H. Supercapacitor performance of MnO_2/$NiCo_2O_4$@N-MWCNT hybrid nanocomposite electrodes. *Journal of Sol-Gel Science and Technology.* 2019; ***91***:154-164.
6. Dhawan S.K, Kumar D, Ram M.K. Application of conducting polyaniline as sensor material for ammonia. *Sens Actuators B Chem* 1997; **40**:99–103.
7. Jinlong L, Meng Y, Suzuki K, Miura H. Fabrication of 3D graphene foam for a highly conducting electrode. Mater Lett. 2017; **196**:369–372
8. Reddy KR, Lee KP, Gopalan AI. Self-assembly approach for the synthesis of electro magnetic functionalized Fe_3O_4/polyaniline nanocomposites: efect of dopant on the properties. Colloids Surf A. 2008; **320**:49–56.
9. Qana A. Alsulami, Laila M. Alharbi, Sherif M.A.S. Keshk. Synthesis of a graphene oxide/$ZnFe_2O_4$/polyaniline nanocomposite and its structural and electrochemical characterization for supercapacitor application. Int J Energy Res. 2021.
10. Song E, Choi J-W. Conducting polyaniline nanowire and its applications in chemiresistive sensing. Nanomaterials. 2013; **3**:498–523.
11. Wei H, Zhu J, Wu S. Electrochromic polyaniline/graphite oxid nanocomposites with endured electrochemical energy storage. Polymer. 2013; **54:**1820–1831.
12. Tengku Nur Atiqah Bt Tengku Ab Mutalib, Soo Jin Tan, Kai Loong FooYun Ming Liew, Cheng Yong Heah, Mohd Mustafa Al Bakri Abdullah. Properties of polyaniline/graphene oxide (PANI/GO) composites: efect of GO loading. Polymer Bulletin. 2021; **78:**4835–4847.
13. Zhu J, Chen M, Qu H. Interfacial polymerized polyaniline/graphite oxide nanocomposites toward electrochemical energy storage. Polymer. 2012; 53:5953–596.

14. Jiang X, Lou S, Chen D. Fabrication of polyaniline/graphene oxide composite for graphite felt electrode modifcation and its performance in the bioelectrochemical system. J Electroanal Chem. 2015; 744:95–100.
15. Crowley K, Smyth MR, Killard AJ, Morrin A Printing polyaniline for sensor applications. Chem Pap. 2013; 67:771–780.
16. Crowley K, Smyth MR, Killard AJ, Morrin A Printing polyaniline for sensor applications.Chem Pap. 2013; 67:771–780.
17. Lei W, Si W, Xu Y, Gu Z,Hao Q. Conducting polymer composites with graphene for use in chemical sensors and biosensors. Microch. Acta. 2014; 181:707–722.
18. Dakshayini BS, Reddy KR, Mishra A. Role of conducting polymer and metal oxide-based hybrids for applications in ampereometric sensors and biosensors. Microchem J. 2019; 147:7–24.
19. Wang H, Lin J, Shen ZX. Polyaniline (PANi) based electrode materials for energy storage and conversion. J Sci Adv Mater Devices 2016; 1:225–255.
20. Dharupaneedi SP, Anjanapura RV, Han JM, Aminabhavi TM (2014) Functionalized graphene sheetsembedded in chitosan nanocomposite membranes for ethanol and isopropanol dehydration via pervaporation. Ind Eng Chem Res 2014; 53:14474–14484.
21. Suhas DP, Raghu AV, Jeong HM, Aminabhavi TM. Graphene-loaded sodium alginate nanocomposite membranes with enhanced isopropanol dehydration performance via a pervaporation technique. RSC Adv. 2013; 3:17120–17130.
22. Suhas DP, Aminabhavi TM, Jeong HM, Raghu AV. Hydrogen peroxide treated graphene as an efective nanosheet fller for separation application. RSC Adv. 2015; 5:100984–100995.
23. Reddy KR, Sin BC, Yoo CH. Coating of multiwalled carbon nanotubes with polymer nanospheres through microemulsion polymerization. J Colloid Interface Sci. 2009 340:160–165.
24. Jinlong L, Meng Y, Suzuki K, Miura H. Fabrication of 3D graphene foam for a highly conducting electrode. Mater Lett. 2017; 196:369–372.
25. Reddy KR, Sin BC, Ryu KS. In situ self-organization of carbon black–polyaniline composites from nanospheres to nanorods: synthesis, morphology, structure and electrical conductivity. Synth Metals. 2009; 159:1934–1939.
26. Chang J, Zhou G, Christensen E R , Heideman R , Chen J. Graphene-based sensors for detection of heavy metals in water: a review. Anal.Bioanal. Chem. 2014; 406:3957–3975.
27. Deshmukh M A, Celiesiute R, Ramanaviciene A, Shirsat M D. EDTA_PANI/SWCNTs nanocomposite modified electrode for electrochemical determination of copper (II), lead (II) and mercury (II) ions. Electroch. Acta . 2018; 259:930–938.
28. Manasi Mahadik, Harshada Patil, Gajanan Bodkhe, Nikesh Ingle, Pasha Sayyad, Theeazen Al-Gahaouri, Sumedh M. Shirsat and Mahendra Shirsat. EDTA Modified PANI/GO Composite Based Detection of Hg (II) Ions. Frontiers in Materials. 2020; 7:81-88.
29. Chernysheva D, Pudova L, Popov Y, Smirnova N, Maslova O, Allix M, Rakhmatullin Leontyev A N, Nikolaev A, Leontyev L. Non-Isothermal Decomposition as Efficient and Simple Synthesis Method of NiO/C Nanoparticles for Asymmetric Supercapacitors. *Nanomaterials*. 2021; *11*:187
30. A. Eftekhari L, Li Y, Yang. Polyaniline supercapacitors. *J. Power Sources* 2017; *347*: 86-107.

31. Chauhan NPS, Mozafari M, Chundawat NS, Meghwal K, Ameta R, Ameta SC. High-performance supercapacitors based on polyaniline–graphene nanocomposites: Some approaches, challenges and opportunities. *J. Industrial and Engineering Chemistry*. 2016;36:13-29.
32. Zhang K, Li Zhang L, S. Zhao X, Wu J. Graphene/Polyaniline Nanofiber Composites as Supercapacitor Electrodes. *Chemistry of Materials*. 2010;22:1392-1401.
33. Salunkhe RR, Hsu SH, Wu KCW, Yamauchi Y. Large-scale synthesis of reduced graphene oxides with uniformly coated polyaniline for supercapacitor applications. *Chem SusChem.* 2014;7:1551-1556.
34. Hou M, Xu M, Hu Y, Li B. Nanocellulose incorporated graphene/polypyrrole film with a sandwich-like architecture for preparing flexible supercapacitor electrodes. *Electrochimica Acta.* 2019;313:245-254.
35. Dong L, Xu C, Li Y, et al. Breathable and Wearable Energy Storage Based on Highly Flexible Paper Electrodes. *Advanced Materials*. 2016;28:9313-9319.
36. Wang Z, Tammela P, Strømme M, Nyholm L. Cellulose-based Supercapacitors: Material and Performance Considerations. *Advanced Energy Materials*. 2017;7.
37. Sun W, Gao G, Zhang K, Liu Y, Wu G. Self-assembled 3D N-CNFs/V2O5 aerogels with core/shell nanostructures through vacancies control and seeds growth as an outstanding supercapacitor electrode material. *Carbon*. 2018;132:667-677.
38. Zhao D, Zhu Y, Cheng W, Chen W, Wu Y, Yu H. Cellulose-Based Flexible Functional Materials for Emerging Intelligent Electronics. *Advanced Materials*. 2021;33.
39. Claro FC, Matos M, Jordão C, Avelino F, Lomonaco D, Magalhães WLE. Enhanced microfibrillated cellulose-based film by controlling the hemicellulose content and MFC rheology. *Carbohydrate Polymers*. 2019;218:307-314.
40. Tokarev I, Minko S. Stimuli-responsive hydrogel thin films. *Soft Matter*. 2009;5:511-524.
41. Rußler A, Sakakibara K, Rosenau T. Cellulose as matrix component of conducting films. *Cellulose*. 2011;18:937-944.
42. Xu Z, Wang T, Wang L, et al. Aniline-grafting graphene oxide/polyaniline composite prepared via interfacial polymerization with high capacitive performance.*J. of Energy Research*. 2019;43(13):7693-7701.
43. Li Y, Xia Z, Gong Q, et al. Green synthesis of free standing cellulose/graphene oxide/polyaniline aerogel electrode for high-performance flexible all-solid-state supercapacitors. *Nanomaterials*. 2020;10:1-18.
44. Zhang X, Zhao J, Xia T, et al. Hollow polypyrrole/cellulose hydrogels for high-performance flexible supercapacitors. *Energy Storage Materials*. 2020;31:135-145.
45. He X, Xiao Q, Lu C, et al. Uniaxially aligned electrospun all-cellulose nanocomposite nanofibers reinforced with cellulose nanocrystals: Scaffold for tissue engineering. *Biomacromolecules*. 2014;15:618-627.
46. Bhadra S, Singha NK, Khastgir D. Polyaniline by new miniemulsion polymerization and the effect of reducing agent on conductivity. *Synthetic Metals*. 2006;156:1148-1154.

47. Wei Y, F. Hsueh K, Way Jang G. A study of leucoemeraldine and effect of redox reactions on molecular weight of chemically prepared polyaniline. *Macromolecules*. 2002;27:518-525.

48. Abdiryim T, Jamal R, Nurulla I. Doping effect of organic sulphonic acids on the solid-state synthesized polyaniline.J.*Applied Polymer Science*. 2007;105:576-584.

49. Ameen S, Akhtar MS, Shin HS. Hydrazine chemical sensing by modified electrode based on in situ electrochemically synthesized polyaniline/graphene composite thin film. *Sensors and Actuators, B: Chemical*. 2012;173:177-183.

50. Liu R, Ma L, Huang S, Mei J, Xu J, Yuan G. A flexible polyaniline/graphene/bacterial cellulose supercapacitor electrode. New Journal of Chemistry. 2017;41(2):857-864.

51. Gong Q, Li Y, Liu X, Xia Z, Yang Y. A facile preparation of polyaniline/cellulose hydrogels for all-in-one flexible supercapacitor with remarkable enhanced performance. Carbohydrate Polymers. 2020;245.

52. Sahoo S, Zhang S, Shim JJ. Porous Ternary High Performance Supercapacitor Electrode Based on Reduced graphene oxide, NiMn2O4, and Polyaniline. Electrochimica Acta. 2016;216:386-396.

53. Li W, Lu H, Zhang N, Ma M. Enhancing the Properties of Conductive Polymer Hydrogels by Freeze-Thaw Cycles for High-*Performance Flexible Supercapacitors*. 2017